RSC Advances

PAPER

View Article Online
View Journal | View Issue

Cite this: *RSC Adv.*, 2022, **12**, 30270

Negatively-charged supported lipid bilayers regulate neuronal adhesion and outgrowth†

Chiara Ausilio,[a] Claudia Lubrano,[abcd] Anna Mariano[a] and Francesca Santoro *[acd]

One of the main challenges in neuroelectronics is the implementation of electronic platforms able to secure a tight coupling with neuronal cells and achieve an optimal signal to noise ratio during stimulation/recording of electrophysiological activity. In this context, supported lipid bilayers (SLBs), recapitulating the structure and the dynamicity of the biological plasma membrane, offer a promising biomimetic approach to trick cells to recognize a device as part of their native environment, tightening the cell-chip coupling. Among possible functionalization strategies used to improve cell adhesion on SLBs, the modification of the bilayer surface charge has been exploited to enhance the electrostatic interaction between the artificial membrane and its biological counterpart. In this work, several SLBs with different lipidic composition were synthesized and interfaced with primary neurons. Starting from a neuron-inspired biomembrane, the negative charges were increased through the addition of 1,2-dipalmitoyl-*sn*-*glycero*-3-phosphoethanolamine-*N*-(succinyl) (succinyl-PE), a lipid exposing phosphate (PO_4^-) groups; furthermore, the reactivity of the succinyl carboxylate group enabled the subsequent addition of negatively charged sulfonate (SO_3^-) groups. The synthesized SLBs were then tested as platforms for neuronal adhesion and network formation. Despite the expected repulsive electrostatic interactions, our work suggests that negatively charged SLBs may influence neurite elongation and branching, highlighting the potential of surface charge to tune neuronal processes at the neuron–SLB interface.

Received 17th August 2022
Accepted 14th October 2022

DOI: 10.1039/d2ra05147h

rsc.li/rsc-advances

Introduction

The development of effective neuroelectronic interfaces able to stimulate and record neuronal activity has always represented a challenge in the bioelectronic field.[1] In this context, in order to promote the seamless integration of electronic devices within biological tissues and therefore achieve an efficient coupling between neurons and their artificial counterpart, several surface engineering approaches have been implemented.[2] For instance, taking inspiration from the biological world, biomimetic chemical functionalization with components of the extracellular matrix (ECM) (*e.g.*, fibronectin, laminin and collagen), providing anchor points to interfacing cells, may be used to promote receptor-mediated cell adhesion to the substrate.[3–7] In addition, charged synthetic polymers can facilitate the attachment of neuronal cells to a substrate.[6] For instance, poly-lysine, a positively charged polymer, modulates cell adhesion *via* a non-receptor-mediated mechanism, interacting electrostatically with the negatively charged cellular membrane.[8,9] Additionally, a few studies have also investigated the ability of negatively charged surfaces to guide neuronal behaviour: for example the presence of carboxylate and sulfonate groups has been identified as highly beneficial for the development of hippocampal neuronal network.[10–12] However, the aforementioned approaches still hardly resemble the extreme complexity and dynamicity of the ECM and cell native environment, in which a plethora of ECM and cell ligands is not statically presented to surrounding cells but is instead integrated within much more fluid neighbouring cell membranes. In this scenario, supported lipid bilayers (SLBs), artificial biomembranes able to mimic the structure and the dynamicity of the biological plasma membrane, have found wide application in bioelectronics.[13] Cells in fact would recognize such synthetic lipid leaflets as part of their native environment, thus securing tighter cell–substrate interactions.[14,15] Previous works reported on the role of positive surface charges in synthetic membranes as a successful strategy to tighten the electrostatic interaction between biological and artificial membranes. In this context, it is now widely known that cationic lipids can successfully support neuronal adhesion.[16] However, in order to understand the influence of surface charge on neuronal growth, we explored the effects of negative charges incorporated within artificial membranes on neuronal adhesion and network formation, combining SLBs dynamicity with the ability of negative charges to guide neuronal behavior.

[a]*Tissue Electronics, Istituto Italiano di Tecnologia, 80125 Napoli, Italy*
[b]*Dipartimento di Chimica, Materiali e Produzione Industriale, Università di Napoli Federico II, 80125, Naples, Italy*
[c]*Faculty of Electrical Engineering and Information Technology, RWTH Aachen, 52074, Germany*
[d]*Institute for Biological Information Processing-Bioelectronics, IBI-3, Forschungszentrum Juelich, 52428, Germany. E-mail: f.santoro@fz-juelich.de*

† Electronic supplementary information (ESI) available. See DOI: https://doi.org/10.1039/d2ra05147h

Remarkably, as the presence of negatively-charged carboxylate and sulfonate groups on glass are highly beneficial for the development of neuronal networks, it is not as unexpected that the negatively charged SLBs may also encourage neuronal cell adhesion.

Several lipid compositions were investigated: firstly, a neuron-inspired biomembrane was synthesized combining 1-palmitoyl-2-oleoyl-*sn-glycero*-3-phosphocholine (POPC), sphingomyelin (SM) and cholesterol (chol), the major components of the neuronal membrane.[17,18] Such membrane was then further functionalized by incorporating the anionic 1,2-dipalmitoyl-*sn-glycero*-3-phosphoethanolamine-*N*-(succinyl) (succinyl-PE) lipid in order to evaluate the role of its negatively charged groups on neuronal behavior. Our findings may provide useful insights on how SLB-based neurointerfaces may be used to secure a tight coupling between neuronal cells and artificial devices, promoting their seamless integration.

Materials and methods

Supported lipid bilayers (SLBs) synthesis

Liposomes were prepared by dissolving lipids in chloroform (Merck, Germany) at the desired concentration (10 mg ml^{-1}). Then, the chloroform was evaporated under a nitrogen stream and by placing the mixture in a desiccator under vacuum for 2 hours to remove any trace of the solvent. The lipid film was rehydrated with phosphate buffered saline (PBS, Sigma Aldrich, USA) at pH 7.4 to achieve the final concentration of 5 mg ml^{-1}. The solution was gently vortexed and then sonicated on ice for 25 minutes. The small unilamellar vesicles (SUVs) were obtained by the extrusion through a polycarbonate membrane with a pore size of 0.1 μm (Merck, Germany) by using a mini extruder (Sigma-Aldrich, USA). The obtained lipid vesicle solution was stored at 4 °C. Prior the SLB formation, the glass cover-slips (Thermo Fisher scientific, USA) were treated with oxygen plasma (Diener Electronic, Germany) for 5 minutes with 50 W at 0.8 mbar pressure. Then, the vesicle solution was diluted to a final concentration of 0.3 mg ml^{-1} with PBS. Lipid bilayers were formed on glass using the vesicle fusion (VF) method, incubating SUVs for 1 h at room temperature. Residual unbounded vesicles were removed with PBS washes. Twelve lipid bilayer compositions were formed with all the possible combinations using 2-oleoyl-1-palmitoyl-*sn-glycero*-3-phosphocholine (POPC), cholesterol (chol), brain sphingomyelin (SM), 1,2-dioleoyl-*sn-glycero*-3-phosphoethanolamine-*N*-(succinyl) (succinyl-PE). All lipids were obtained from Sigma-Aldrich, USA. The lipids mixture consists of fixed 20% (w/w) of succinyl-PE and 0.5% (w/w) of Texas Red™ 1,2-dihexadecanoyl-*sn-glycero*-3-phosphoethanolamine, triethylammonium salt (Texas Red™ DHPE, Thermo Fisher scientific, USA), with POPC, cholesterol and sphingomyelin at a molar ratio of (1 : 1 : 1).

EDC/NHS reaction

The activation of the carboxylic groups of succinyl-PE was performed after the lipid vesicles were vortexed. Immediately before the experiment, 50 μl of EDC (Sigma-Aldrich, USA) (60 mg ml^{-1} solution in pH 5.7 PBS buffer) and 50 μl of NHS (Abcam, UK) (50 mg ml^{-1} solution in pH 5.7 PBS buffer) were added to 200 μl of lipid vesicles solution to convert the carboxyl groups of succinyl-PE lipid to chemically active NHS-ester group. The resulting lipid mixture was extruded through a polycarbonate membrane with a pore size of 0.1 μm by using a mini extruder. After the plasma treatment, the glass coverslips were incubated with the vesicle solution at a concentration of 0.3 mg ml^{-1} for 1 hour. The unbounded vesicles were removed with PBS washes.

Quantification of surface charge

The surface charge of PLL-coated glasses and SLBs was compared by using fluorescently labelled amine-modified latex beads (Sigma Aldrich, USA) (excitation/emission of 481/644 nm). The beads solution was diluted to a final concentration of 0.5 mg ml^{-1} in PBS. The substrates were incubated for 10 minutes at room temperature and then washed with PBS. Images were acquired at Axio Vario microscope (Zeiss, Germany) with 63× water immersion objective. The ImageJ software was used to count the bounded beads on the surface of the substrates.

Fluorescence recovery after photobleaching (FRAP) characterization

A Leica TCS SP5 gated with stimulated emission depletion (STED) (Germany) was used for FRAP measurements. The Texas Red DHPE lipid was included in the lipid precursor solution to fluorescently label the lipid bilayers. The images were acquired by using a 25× water immersion objective with scanning speed of 1000 Hz. A circular region with a diameter of 20 μm was bleached using a 114 mW 592 nm laser beam for 1.3 seconds. The recovery of the fluorescence of the bleached spot was monitored for 5 minutes. The fluorescence intensity was normalized to a reference spot in each measurement and fit with a Bessel function. The images were processed with ImageJ software (NIH, USA) through radial profile tool to quantify the recovery of the fluorescence along the radius of the selected area. Three independently bilayers were prepared and imaged for each composition. The diffusion coefficient was calculated through the following formula:

$$D = \omega^2/(4\tau_{(1/2)})$$

with ω radius of the bleached area and $\tau_{1/2}$ the time required to achieve half of the maximum recovery intensity.

Atomic force microscopy (AFM) characterization

Bruker Dimension Icon microscope (Bruker Corporation, USA) was used for AFM measurements. AFM images were collected in ScanAsyst mode in hydrated condition by using the ScanAsyst-Fluid probe (Bruker Corporation, USA), with a spring constant of 0.7 N m^{-1}, a tip radius of 5–20 nm, and resonance frequency of 150 kHz. The imaging force was approximately 700 pN and the scan rate was typically 1.5 Hz for 256 × 256 pixels images. The gain was optimized to reduce the noise. Three independently bilayers were prepared and imaged for each composition and several areas were scanned for each sample. The software analysis

Nanoscope analysis 2.0 was used to process the images and to calculate the roughness average (R_a) over a 2 μm × 2 μm areas.

Primary neurons culture

Fertilized eggs were purchased from Charles Rivers (USA) and incubated for 9 days at 37 °C. The cortices were obtained from excised chicken embryo brains and maintained in Hibernate-A Medium (Thermo Fisher Scientific, USA) in ice. The tissues were processed with 0.25% trypsin–EDTA (Life Technologies, USA) at 37 °C for 20 minutes. Trypsin was then replaced with Neurobasal medium (Life Technologies, USA) supplemented with 1% B-27 supplement, 1% L-glutamine (CF = 2 mM) (Life Technologies, USA) and 0.2% penicillin–streptomycin (Sigma Aldrich, USA). The number of viable cells was obtained by using the Countess II Automated Cell Counter (Thermo Fisher Scientific, USA). Prior cell plating, the PBS of the SLBs was exchanged with pre-warmed Neurobasal medium without exposing the lipids to air. Glass coverslips, coated with 0.01% poly-L-lysine (PLL, Sigma Aldrich, USA), were used as control samples.

Biocompatibility assay of cortical neurons

The investigation of the primary cortical neurons' viability was performed by using calcein-AM (1 : 1000 in PBS) (Sigma Aldrich, USA) and the Live/Dead Fixable Violet Dead Cell Stain Kit (1 : 1000 in PBS) (Life Technologies, USA). At 1 day *in vitro* (DIV), the primary cortical neurons were incubated with both staining solutions for 20 minutes at room temperature and then washed with PBS three times. Images of live (green fluorescent signal) and dead (blue fluorescent signal) cells were obtained with an Axio Vario microscope (Zeiss, Germany) using a 20× water immersion objective. ImageJ software was used to perform cell counting of live and dead cells populations.

The % viability was calculated using the following formula:

$$\%\ \text{viability} = (\text{viable cells}/(\text{viable} + \text{dead cells})) \times 100$$

Three lipid bilayer samples were formed for each composition per experiment. Viability was determined by acquiring 5 frames per experiment from 3 independent cell preparations ($N = 3$).

Immunocytochemistry

At 4 DIV primary cortical neurons were fixed with 4% paraformaldehyde (Società Italiana Chimici, Italy) in PBS solution (pH 7.2) at room temperature for 20 minutes and washed with PBS three times. Then, the fixed cells were incubated with 0.1% Triton X-100 (Merck, Germany) for 5 minutes, to permeabilize the cellular membrane, and washed with PBS three times. The samples were incubated with 2% bovine serum albumin (Sigma-Aldrich, USA) for at least 45 minutes at room temperature to prevent the un-specific binding of the antibodies. Next, the cells were incubated with the prepared primary antibody solution for 1 hour at room temperature, followed by the 2% BSA washing steps. Anti-βIII-tubulin primary antibody (mouse, final concentration 1 μg ml^{-1} in 2% BSA) (Abcam, UK) was used to label microtubules. Alexa Fluor 647 (anti-mouse, $\lambda_{EX/EM}$ = 650/671 nm) (Life Technologies, USA) secondary antibody for anti-βIII-tubulin was diluted (1 : 500 dilution, CF = 2 μg ml^{-1} in 2% BSA) and incubated for 30 minutes at room temperature. After washing with 2% BSA three times, cell nuclei were labelled with Hoechst 33342 (1 : 5000 dilution, $\lambda_{EX/EM}$ = 361/497 nm) (Thermo Fisher Scientific, USA) for 10 minutes at room temperature. Finally, the samples were washed three times with PBS and protect from light until imaging. Images were acquired at Axio Vario microscope (Zeiss, Germany) with 40× water immersion objective. The NeuronJ plugin in the ImageJ software was used to measure in semi-automated way the number and the length of the neurites. NeuronJ was also used to classify neurites in primary (when linked the cell body), secondary (when starting from a primary neurite) and tertiary (when starting from a secondary neurite).

A neuronal node is defined as the site of branching of secondary and tertiary neurites. The normalized length and number of neurites and the normalized number of nodes were obtained using the following formulas:

$$\text{Normalized neurites length} = (\text{total neurites length})/(\text{total cell number})$$

$$\text{Normalized neurites number} = (\text{total neurites number})/(\text{total cell number})$$

$$\text{Normalized number of nodes} = (\text{total number of nodes})/(\text{total cell number})$$

The percentage of length and numbers of primary, secondary and tertiary neurites were obtained using the following formula:

$$\%\ \text{primary neurites length} = (\text{primary neurites length})/(\text{total neurites length}) \times 100$$

$$\%\ \text{primary neurites number} = (\text{primary neurites number})/(\text{total neurites number}) \times 100$$

Statistical analysis

For the cell viability and the neurite number and length, all the data is plotted as mean ± standard deviation (SD). The statistical analysis was performed using GraphPad Prism 8. A one-way Anova with a Tukey-*post hoc* test was performed to evaluate any effect of the SLBs used on the percentage of live cells compared to glass. The same statistical analysis was performed to evaluate any SLBs-induced effect on neurites branching and elongation compared to glass. Significance was established at p-value < 0.05.

Results and discussion

SLBs fluidity and surface morphology characterization

In this work artificial lipid bilayers were synthetized starting from a ternary mixture of POPC, cholesterol and

sphingomyelin, the major components of neuronal membranes: such composition including zwitterionic lipids (Fig. S1†) displays a neutral surface charge.[17–19] The negatively charged succinyl-PE (succ-PE) lipid, presenting an unbalanced PO_4^- group (Fig. S1†), was also incorporated in the SLBs. Moreover, the carboxylic group present on the succinyl-PE lipid head was converted into an into an NHS-ester group (Fig. S1†), through an EDC/NHS (1-ethyl-3-(3-dimethylaminopropyl)-carbodiimide/*N*-hydroxy-sulfo-succinimide sodium salt) mediated reaction.[20] Therefore, three different compositions were obtained as shown in Fig. 1A: a neutral biomembrane (Fig. 1A(i)), a succinyl-PE-containing SLB with its PO_4^- groups (Fig. 1A(ii)), and a sulfo-NHS–succinyl-PE-containing bilayer with PO_4^- and SO_3^- groups (Fig. 1A(ii)). Additionally, several mixtures obtained from either two or three lipids (POPC, cholesterol and sphingomyelin) were also investigated. SLBs were formed on glass by vesicle fusion (VF);[21] briefly, the substrates were activated by oxygen plasma treatment and incubated with lipid vesicles at a critical concentration to induce rupture. In the case of the bilayer containing sulfo-NHS–succinyl-PE, the functionalization was performed prior vesicles deposition.

After the bilayer formation, the surface charge was investigated by using fluorescent positively-charged amine-modified latex beads, exploring the interaction between the positive charges of the beads and the charges of the SLBs.

As expected, positively charged PLL-coated glasses did not show any fluorescence, owing to the repulsive action of the amino group of the polymer against the bead's amine (Fig. S2(i)†). Similarly, neutral SLBs did not display the presence of fluorescent signal confirming the absence of charged groups (Fig. S2(ii)†). Remarkably, negatively charged SLBs showed the presence of bright spots due to the binding of the negatively phosphate and sulfonate groups of the SLBs with the positively charged amine groups of the beads (Fig. S2(iii and iv)†), suggesting that in the presence of succinyl-PE, SLBs are indeed negatively charged.

Then, the correct formation and fluidity of the various lipid bilayers were evaluated by means of fluorescent recovery after photobleaching (FRAP).[22] All investigated compositions showed the complete recovery of fluorescence in a photobleached spot after 5 minutes (Fig. 1B and S3†), suggesting that the SLB-embedded lipids display a high lateral mobility. Indeed, these results were further confirmed by the estimation of the

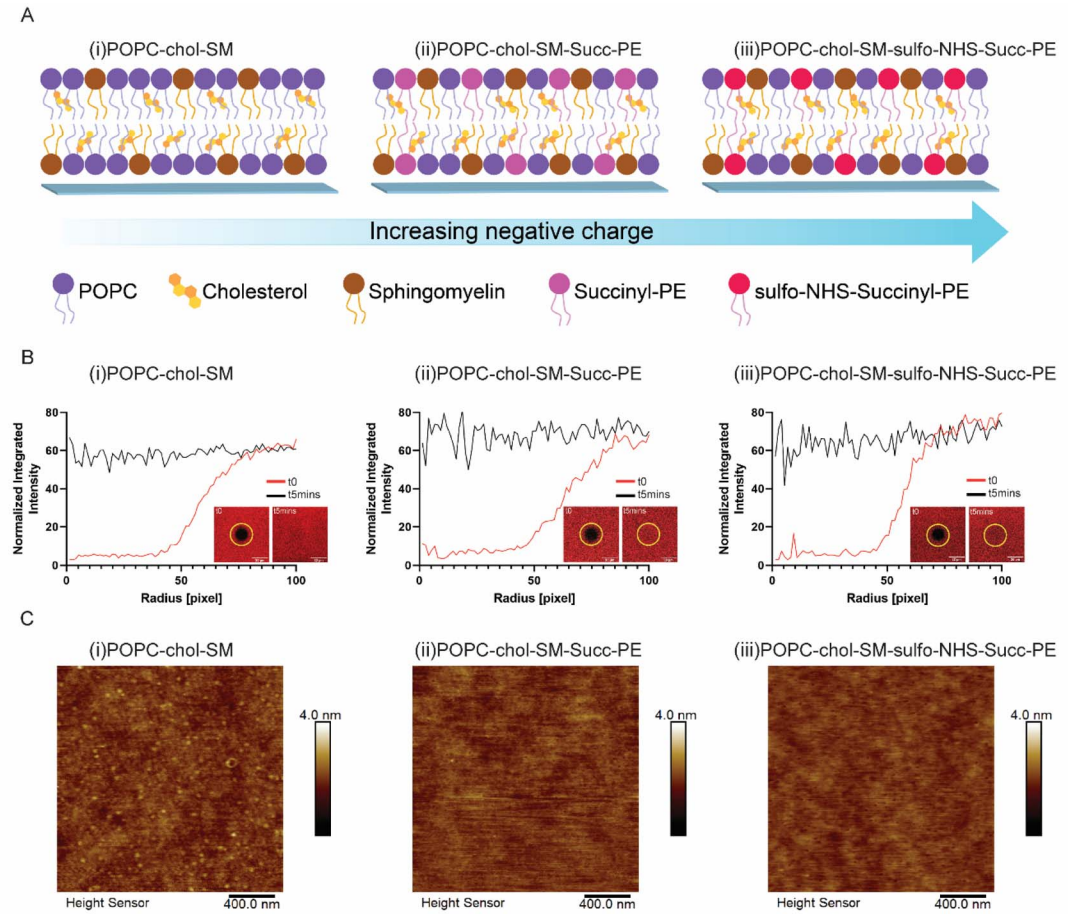

Fig. 1 SLBs fluidity and surface morphology characterization of SLBs with increasing negative surface charges. (A) Schematic representation of (i) the neuron-inspired SLB, (ii) the succinyl-PE containing SLB and (iii) the sulfo-NHS/succinyl-PE-containing SLB. (B) Normalized fluorescence intensity profiles of (i) POPC/chol/SM, (ii) POPC/chol/SM/succ-PE and (iii) POPC/chol/SM/sulfo-NHS–succ-PE and the corresponding FRAP image; the recovery of the fluorescence intensity in the photobleached area is shown at $t = 0$ and 5 minutes. (C) AFM images of (i) POPC/chol/SM, (ii) POPC/chol/SM/succ-PE and (iii) POPC/chol/SM/sulfo-NHS–succ-PE.

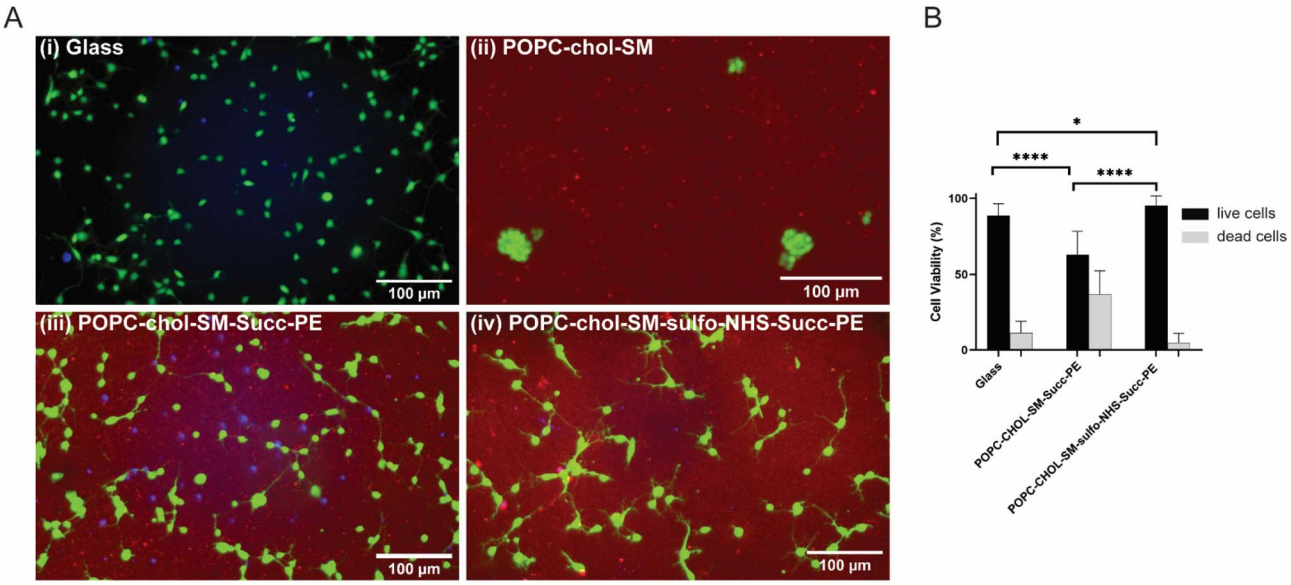

Fig. 2 The effect of SLBs surface charge on neurons viability. (A) Fluorescence images of cortical neurons cultured on (i) PLL-coated glass, (ii) POPC/chol/SM, (iii) POPC/chol/SM/succ-PE and (iv) POPC/chol/SM/sulfo-NHS–succ-PE at 1 DIV. Live cells are showed in green, dead cells in blue and SLBs in red. (B) Percentage of live cells are reported as mean ± SD ($n = 3$), * = $p < 0.05$, ** = $p < 0.01$, *** = $p < 0.001$, **** = $p < 0.0001$.

diffusion coefficients, which rely on SLBs fluidity (Table S1†). Interestingly, only when cholesterol is incorporated in sulfo-NHS–succinyl-PE-containing membranes, the diffusion coefficient was reduced. This may be due to the intercalation of the sterol between the unsaturated lipids' chains which has a significant ordering effect influencing membrane fluidity.[23] Additionally, the presence of sulfo-NHS-ester bound to the head of succinyl-PE lipid might cause the reduction of lipid's mobility inside the membrane, as hinted by the decreased diffusion coefficient. Afterwards, an extensive characterization of the formation and homogeneity of lipid bilayers has been carried out by means of atomic force microscopy (AFM) measurements in aqueous condition.[24] Such technique allows the characterization of phase separated domains within complex mixtures of lipids.[25] In agreement with previous works,[26] SLBs showed smooth and homogeneous surface morphologies (Fig. 1C and S4†), demonstrating relatively defect-free surfaces. In particular, when SM is present in the SLBs (Fig. 1C(i) and S4†), but not succinyl-PE, SLBs mainly displayed a granular surface.[27] Indeed, the incorporation of succinyl-PE lipid resulted in a flattening of the surface (Fig. 1C(ii, iii) and S4†). Notably, the incorporation of the cholesterol did not cause a phase separation (Fig. 1C and S4†), suggesting that the membranes are in a single-phase mode at the temperature of the experiments.[25] Furthermore, the average roughness (R_a) of the various SLBs was estimated (Table S1†). R_a values ranged between 120 and 170 pm, suggesting that the homogeneity and the smoothing of SLBs surfaces was not dependent on the lipid mixtures.

Evaluation of primary neurons viability on SLBs

In order to evaluate the biocompatibility of SLBs with primary cortical neurons after 1 DIV, live and dead cells were fluorescently labelled with calcein-AM (in green) and Live/Dead Fixable Violet Dead Cell Stain Kit (in blue), respectively (Fig. 2A(i–iv)). Fluorescence micrographs showed nicely spreading and elongating neurons on PLL-coated glasses (Fig. 2A(i)) and on the negatively charged succinyl-PE-containing SLBs (Fig. 2A(iii, iv) and S5†), while neuronal clusters were observed on the neutral SLBs (Fig. 2A(ii) and S5†), suggesting that the lack of surface charge might indeed hinder neuronal adhesion.[28] Interestingly, primary neurons displayed good viability on the sulfo-NHS–succinyl-PE-SLBs, with a high percentage of live cells (~95%), comparable to the percentage measured for PLL-coated glasses, whereas succinyl-PE-containing SLBs exhibited significantly lower cells' viability (Fig. 2B). In agreement with previous works,[10] these results confirmed the importance of negatively charged surfaces to support neuronal adhesion, in particular highlighting the beneficial impact of PO_4^- and SO_3^- groups of succinyl-PE lipid.

Neurite elongation and branching on SLBs

In order to investigate the effect of negatively charged SLBs on neurite elongation and branching, succinyl-PE and sulfo-NHS–succinyl-PE-containing membranes were interfaced with primary neurons. After 4 DIV, cells were fluorescently labelled for nuclei (in blue) and β-III tubulin (in red) (Fig. 3A(i–iii) and S6†). Here, neurons with elongated neurites were found either on positively PLL-coated control glasses (Fig. 3(i)) and on negatively SLBs containing succinyl-PE and sulfo-NHS–succinyl-PE lipids (Fig. 3(ii, iii) and S6†). This is in agreement with previous works showing stable neuronal adhesion on charged substrates.[10–12,29] Conversely, the neutral SLB composition did not support neuronal growth and thus was not further investigated.[30] Interestingly, sulfo-NHS–succinyl-PE-SLBs encouraged

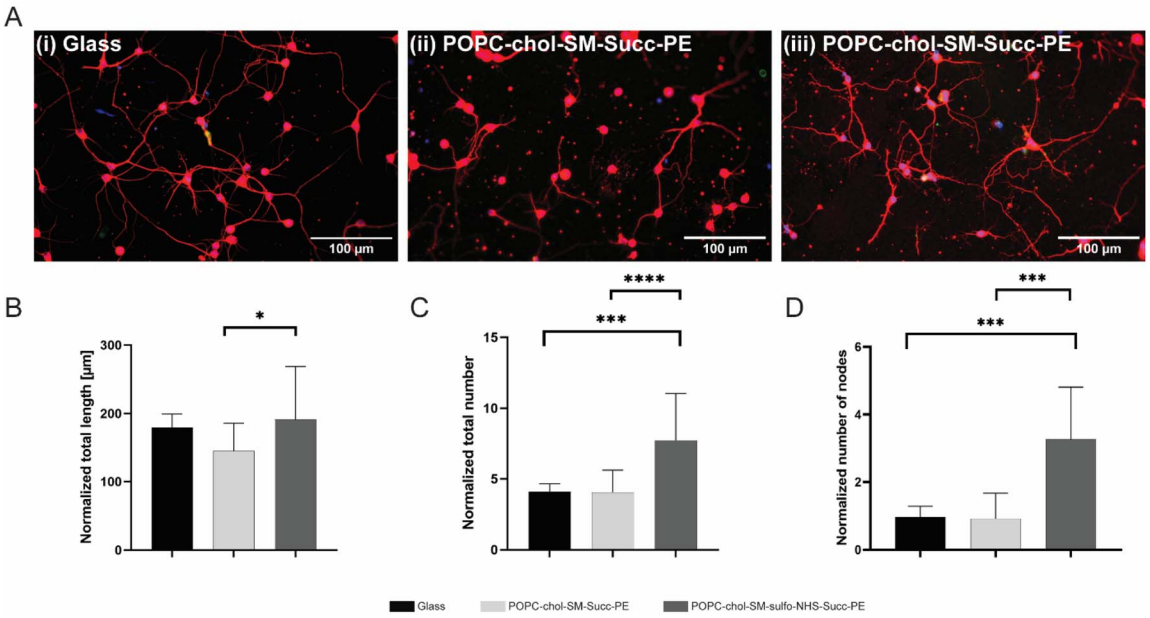

Fig. 3 SLBs-mediated neurite elongation and branching. (A) Fluorescence micrographs of cortical neurons on (i) PLL-coated glass, (ii) POPC/chol/SM/succ-PE and (iii) POPC/chol/SM/sulfo-NHS–succ-PE at 4 DIV. In particular, red fluorescence signal to βIII-tubulin associated elements and blue signal to Hoechst identifying the nuclei. (B) Quantification of normalized neurites length. (C) Quantification of normalized number of neurites. (D) Quantification of normalized number of neuronal nodes. Normalized values reported as mean ± SD ($n = 3$), * = $p < 0.05$, *** = $p < 0.001$, **** = $p < 0.0001$.

neurites elongation resulting in significantly higher neurites length (191.2 ± 77.2 µm, $n = 3$) compared to succinyl-PE containing membranes (145 ± 40.7 µm, $n = 3$) (Fig. 3B and S6B†), suggesting that the incorporation of SO_3^- groups may indeed promote neurite elongation.[11] The neuronal network was then examined by counting the total number of neurites and the number of nodes, the branching sites along elongating neurites. Notably, the normalized number of neurites was

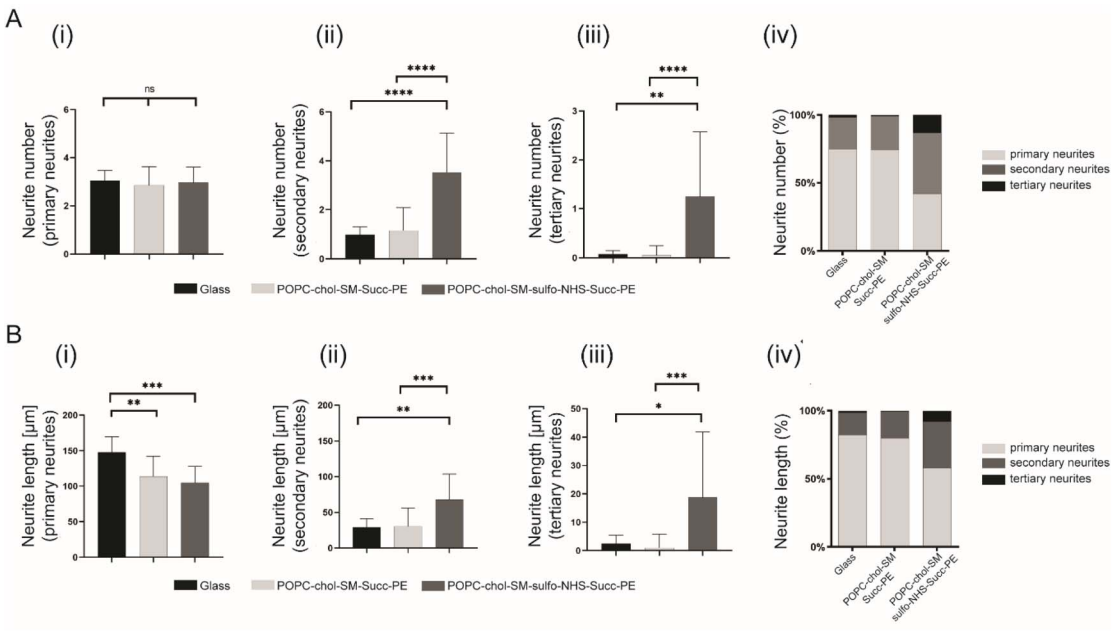

Fig. 4 The effect of SLBs on neurite arborization. (A) Normalized number of (i) primary, (ii) secondary and (iii) tertiary neurites reported as mean ± SD ($n = 3$), ns = not significant * = $p < 0.05$, ** = $p < 0.01$, *** = $p < 0.001$, **** = $p < 0.0001$. (iv) Percentage of primary, secondary and tertiary neurite across each substrate. (B) Normalized length of (i) primary, (ii) secondary and (iii) tertiary neurites reported as mean ± SD ($n = 3$), ns = not significant * = $p < 0.05$, ** = $p < 0.01$, *** = $p < 0.001$, **** = $p < 0.0001$. (iv) Percentage of primary, secondary and tertiary neurite across each substrate.

significantly lower on PLL-coated-glass and succinyl-PE-containing SLBs (Fig. 3C and S6C†). Moreover, the number of nodes was significantly higher on sulfo-NHS–succinyl-PE-SLBs (Fig. 3D, S6D and E†). Taken together, these results suggested that the presence of SO_3^- moieties may enhance neurite sprouting, favoring neuronal network arborization.[11]

Then, the effect of the different SLBs composition on neurite elongation and branching, the normalized number of primary, secondary and tertiary neurites as well as their normalized length was studied. Interestingly, the normalized number of primary neurites was not significantly different between PLL-coated control glass and SLBs (Fig. 4A(i)). However, sulfo-NHS–succinyl-PE-containing SLBs promoted the sprouting of secondary and tertiary neurites resulting in significatively increased neurites number compared to succinyl-PE-containing membranes and PLL-coated glass (Fig. 4B(ii, iii) and S7†). Such increased arborization along primary neurites may be due to the presence of SO_3^- moieties promoting neurite initiation.[10,11] This result was also confirmed by the increased percentage of secondary and tertiary neurites numbers when neurons were cultured on SLBs (Fig. 4B(iv) and S7†). These findings were supported by recent studies in which negatively charged groups, such as carboxylate and sulfonate groups, can indeed mediate neuronal adhesion and guide neurites extension and neuronal networks formation.[12] Then, the length of primary, secondary and tertiary neurites was compared across different SLBs. The length of primary neurites was significantly higher on PLL-coated glass (147.8 ± 21.9 μm, $n = 3$) compared to neuronal SLBs containing succinyl-PE (113.5 ± 28.7 μm, $n = 3$) and sulfo-NHS–succinyl-PE (104.6 ± 23.2 μm, $n = 3$) (Fig. 4B(i)). Remarkably, the length of both secondary and tertiary neurites displayed a significative increase after the incorporation of the sulfo-NHS–succinyl-PE (Fig. 4B(ii, iii) and S7†). This was yet confirmed by the percentage of tertiary neurite length measured for sulfo-NHS–succinyl-PE-containing SLBs which was higher than that found both on PLL-coated glass and succinyl-PE-SLBs (Fig. 4B(iv) and S7†). Consistent with previous reports,[10–12] these results suggests that the effect of SO_3^- groups observed in sulfo-NHS–succinyl-PE-containing membranes enhance both the formation and elongation of secondary and tertiary neurites, inevitably influencing neurites sprouting.

Conclusions

To promote the seamless integration of bioelectronic devices within biological tissues, several engineering approaches have been implemented. Among these, charged surfaces have been widely used to mediate the interaction with the cellular membranes. For instance, positively charged polymers as well as glass substrates functionalized with negatively charged carboxylate and sulfonate groups may have beneficial effect on neuronal growth. Recently, a more biomimetic approach based on SLBs has found wide application in bioelectronics recapitulating the structure and the dynamicity of the cellular membrane on rigid substrates in order to secure the cell–material interaction. In this context, it is now known that positively charged SLBs can successfully support neuronal adhesion. However, only fewer studies have investigated the effect of negatively charged membranes on neuronal behavior at the SLB–neuron interface. In this work, we have demonstrated the potential effect of negatively charged SLBs on neuronal adhesion and network formation.

Briefly, starting from a ternary mixture of POPC, cholesterol and sphingomyelin, SLBs were synthesized. Such biomimetic membranes were then functionalized with succinyl-PE, a negatively charged lipid, in order to evaluate the role of its PO_4^- groups on neurite branching and elongation. Furthermore, the presence of negative charges was further increased by converting the carboxylic group of the succinyl-PE lipid into an NHS-ester group, exposing SO_3^- groups on the surface of the membranes. As a results, SLBs containing succinyl-PE and sulfo-NHS–succinyl-PE lipids displayed good biocompatibility with cortical neurons, supporting neuronal adhesion. Remarkably, the incorporation of the sulfo-NHS–succinyl-PE lipid promoted neurites sprouting, inducing a significative increase of the number and the length of both secondary and tertiary neurites. The gathered results highlight the potential of negatively charged SLBs to promote neurites arborization, paving the way towards the development of *in vitro* neuronal biointerfaces able to tune a desired neuronal behaviour at the cell–material interface.

Author contributions

The manuscript was written through contributions of all authors. All authors have given approval to the final version of the manuscript.

Conflicts of interest

The authors declare no conflict of interest.

Acknowledgements

F. S. acknowledges the support of the European Research Council Starting Grant BRAIN-ACT No. 949478.

References

1 S. F. Cogan, Neural Stimulation and Recording Electrodes, *Annu. Rev. Biomed. Eng.*, 2008, **10**, 275–309.
2 A. Mariano and et al, ., Advances in Cell-Conductive Polymer Biointerfaces and Role of the Plasma Membrane, *Chem. Rev.*, 2022, **122**, 4552–4580.
3 X. Li and et al, ., Short Laminin Peptide for Improved Neural Stem Cell Growth, *Stem Cells Transl. Med.*, 2014, **3**, 662–670.
4 A. Zoso, M. Boffito, R. Laurano, I. Carmagnola and V. Chiono, Cell–biomaterial interactions: the role of ligand functionalization, in *Handbook of Biomaterials Biocompatibility*, Elsevier, 2020, pp. 139–173, DOI: 10.1016/B978-0-08-102967-1.00009-8.
5 M. C. Amores de Sousa and et al, ., Functionalization of Electrospun Nanofibers and Fiber Alignment Enhance

Neural Stem Cell Proliferation and Neuronal Differentiation, *Front. Bioeng. Biotechnol.*, 2020, **8**, 580135.

6 S. Rao and J. O. Winter, Adhesion molecule-modified biomaterials for neural tissue engineering, *Front. Neuroeng.*, 2009, **2**(6), DOI: 10.3389/neuro.16.006.2009.

7 D. Lam and et al, ., Tissue-specific extracellular matrix accelerates the formation of neural networks and communities in a neuron-glia co-culture on a multi-electrode array, *Sci. Rep.*, 2019, **9**, 4159.

8 E. Yavin and Z. Yavin, Attachment and Culture of Dissociated Cells from Rat Embryo Cerebral Hemispheres on Polylysine-Coated Surface, *J. Cell Biol.*, 1974, **62**, 540–546.

9 A. K. Vogt, L. Lauer, W. Knoll and A. Offenhausser, Micropatterned Substrates for the Growth of Functional Neuronal Networks of Defined Geometry, *Biotechnol. Prog.*, 2003, **19**, 1562–1568.

10 M.-H. Kim and et al, ., Accelerated Development of Hippocampal Neurons and Limited Adhesion of Astrocytes on Negatively Charged Surfaces, *Langmuir*, 2018, **34**, 1767–1774.

11 V. P. Swarup and et al, ., Exploiting Differential Surface Display of Chondroitin Sulfate Variants for Directing Neuronal Outgrowth, *J. Am. Chem. Soc.*, 2013, **135**, 13488–13494.

12 S. Gilles and et al, ., Control of Cell Adhesion and Neurite Outgrowth by Patterned Gold Nanoparticles with Tunable Attractive or Repulsive Surface Properties, *Small*, 2012, **8**, 3357–3367.

13 A. Svetlova, J. Ellieroth, F. Milos, V. Maybeck and A. Offenhäusser, Composite Lipid Bilayers from Cell Membrane Extracts and Artificial Mixes as a Cell Culture Platform, *Langmuir*, 2019, **35**(24), 8076–8084.

14 J. van Weerd, M. Karperien and P. Jonkheijm, Supported Lipid Bilayers for the Generation of Dynamic Cell-Material Interfaces, *Adv. Healthcare Mater.*, 2015, **4**, 2743–2779.

15 C.-J. Huang and Y.-C. Chang, Construction of Cell–Extracellular Matrix Microenvironments by Conjugating ECM Proteins on Supported Lipid Bilayers, *Front. Mater.*, 2019, **6**, 39.

16 S.-E. Choi, K. Greben, R. Wördenweber and A. Offenhäusser, Positively charged supported lipid bilayer formation on gold surfaces for neuronal cell culture, *Biointerphases*, 2016, **11**, 021003.

17 L. Paoletti, C. Elena, P. Domizi and C. Banchio, Role of Phosphatidylcholine during Neuronal differentiation, *IUBMB Life*, 2011, **63**(9), 714–720.

18 H. I. Ingólfsson and et al, ., Computational Lipidomics of the Neuronal Plasma Membrane, *Biophys. J.*, 2017, **113**, 2271–2280.

19 G. Hussain and et al, ., Role of cholesterol and sphingolipids in brain development and neurological diseases, *Lipids Health Dis.*, 2019, **18**, 26.

20 C.-J. Huang and et al, ., Type I Collagen-Functionalized Supported Lipid Bilayer as a Cell Culture Platform, *Biomacromolecules*, 2010, **11**, 1231–1240.

21 C. A. Keller, K. Glasmästar, V. P. Zhdanov and B. Kasemo, Formation of Supported Membranes from Vesicles, *Phys. Rev. Lett.*, 2000, **84**, 5443–5446.

22 D. Axelrod, D. E. Koppel, J. Schlessinger, E. Elson and W. W. Webb, Mobility measurement by analysis of fluorescence photobleaching recovery kinetics, *Biophys. J.*, 1976, **16**, 1055–1069.

23 S. R. Tabaei and et al, ., Formation of Cholesterol-Rich Supported Membranes Using Solvent-Assisted Lipid Self-Assembly, *Langmuir*, 2014, **30**, 13345–13352.

24 I. Reviakine and A. Brisson, Formation of Supported Phospholipid Bilayers from Unilamellar Vesicles Investigated by Atomic Force Microscopy, *Langmuir*, 2000, **16**, 1806–1815.

25 S. D. Connell and D. A. Smith, The atomic force microscope as a tool for studying phase separation in lipid membranes (Review), *Mol. Membr. Biol.*, 2006, **23**, 17–28.

26 J. Jass, T. Tjärnhage and G. Puu, From Liposomes to Supported, Planar Bilayer Structures on Hydrophilic and Hydrophobic Surfaces: An Atomic Force Microscopy Study, *Biophys. J.*, 2000, **79**, 3153–3163.

27 M.-C. Giocondi, S. Boichot, T. Plénat and C. Le Grimellec, Structural diversity of sphingomyelin microdomains, *Ultramicroscopy*, 2004, **100**, 135–143.

28 D. A. Stenger, C. J. Pike, J. J. Hickman and C. W. Cotman, Surface determinants of neuronal survival and growth on self-assembled monolayers in culture, *Brain Res.*, 1993, **630**, 136–147.

29 D. Kleinfeld, K. Kahler and P. Hockberger, Controlled outgrowth of dissociated neurons on patterned substrates, *J. Neurosci.*, 1988, **8**, 4098–4120.

30 Q. Tu and et al, ., Effects of surface charges of graphene oxide on neuronal outgrowth and branching, *Analyst*, 2014, **139**, 105–115.